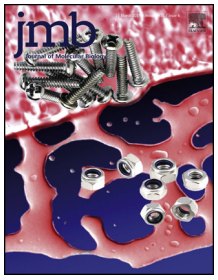

The Molecular Mechanisms Underlying Hidden Phenotypic Variation among Metallo-β-Lactamases

Raymond D. Socha, John Chen and Nobuhiko Tokuriki

Michael Smith Laboratories, *University of British Columbia, Vancouver, BC V6T 1Z4, Canada*

Correspondence to Nobuhiko Tokuriki: *Michael Smith Laboratories, University of British Columbia, Vancouver, BC V6T 1Z4, Canada. tokuriki@msl.ubc.ca*
https://doi.org/10.1016/j.jmb.2019.01.041
Edited by Dan Tawfik

Abstract

Genetic variation among orthologous genes has been largely formed through neutral genetic drift while maintaining the functional role of these genes. However, because the evolution of gene occurs in the context of each host organism, their sequence changes are also associated with adaptation to a specific environment. Thus, genetic variation can create critical phenotypic variation, particularly when genes are transferred to a new host by horizontal gene transfer. Unveiling "hidden phenotypic variation" is particularly important for genes that confer resistance to antibiotics. However, our understanding of the molecular mechanisms that underlie phenotypic variation remains limited. Here we sought to determine the extent of phenotypic variation in the B1 metallo-β-lactamase (MBL) family and its molecular basis by systematically characterizing eight MBL orthologs, including NDM-1 and VIM-2 and IMP-1. We found that these MBLs confer diverse levels of resistance. The phenotypic variation cannot be explained by variation in catalytic efficiency alone; rather, it is the combination of the catalytic efficiency and abundance of functional periplasmic enzyme that best predicts the observed variation in resistance. The level of functional periplasmic expression varied dramatically between MBL orthologs. This was the result of changes at multiple levels of each ortholog's: (1) quantity of mRNA, (2) amount of MBL expressed, and (3) efficacy of functional enzyme translocation to the periplasm. Overall, it is the interaction between each gene and the host's underlying cellular processes (transcription, translation, and translocation) that determines MBL genetic incompatibility through horizontal gene transfer. These host-specific processes may constrain the effective spread and deployment of MBLs to certain host species and could explain the current observed distribution bias.

Introduction

Orthologs are genetically diverged genes that typically perform the same functional role in different host organisms. Traditionally, the genetic variation among orthologs was thought to be largely neutral, or not related to their function. Such variation is acquired through neutral genetic drift, that is, a process in which a purifying selection allows the accumulation of neutral mutations while maintaining physiological function [1]. However, it has recently become apparent that many, if not most, genetic changes are driven by adaptation resulting from, for example, transient historical changes in the level of selection pressure (e.g., pH, temperature, the concentration of nutrients, and antibiotics) [2]. Moreover, some genetic changes may be driven by co-evolution with other proteins and molecules within each organism [3]. While these sequence changes can be neutral within each organism, they can be deleterious or advantageous if the gene is passed to a new host organism through horizontal gene transfer (HGT), revealing "hidden phenotypic variation" [4–7]. Such phenotypic variation is often observed through sub-optimal heterologous protein expression in conventional laboratory hosts such as *Escherichia coli*, which occurs due to incompatibility between the gene and host [8–11]. Moreover, hidden phenotypic variation may play an important role in the evolution and dissemination of antibiotic resistance genes because they are frequently transferred between organisms through HGT

[4,5,12]. However, our understanding of the molecular mechanisms underlying phenotypic variation and genetic incompatibility is still limited.

The B1 metallo-β-lactamase (MBL) family is one such group of antibiotic resistance genes that has disseminated extensively through HGT to a wide variety of bacterial pathogens, causing a serious threat to healthcare systems worldwide [13–16]. Despite high levels of genetic variation (with pairwise amino acid identities as low as 20%), these orthologs feature a shared αββα-fold, an identical active-site architecture (two zinc binding sites coordinated by H-H-H and D-C-H), and the ability to confer resistance to most β-lactam antibiotics by catalyzing the hydrolysis of the β-lactam ring (Fig. 1) [18–20]. Since the first B1 MBL, BcII, was isolated from the genome of *Bacillus cereus* in 1966, MBLs have been identified in a growing number of bacteria that belong to diverse phyla such as Bacteroidetes, Firmicutes, and Proteobacteria [21–25]. However, in the last two decades, some types of MBLs, such as NDM-, VIM-, IMP-, and SPM-type, have become "acquirable" through their association with plasmids and other transferable elements and have subsequently disseminated to diverse clinical pathogens, such as *Pseudomonas aeruginosa*, *Acinetobacter baumanni*, *Klebsiella pneumoniae*, *Enterobacter cloacae*, and *E. coli* [17,19,26–28]. These observations lead to a series of questions regarding phenotypic variation among MBLs and antibiotic resistance in pathogens: How might phenotypic variation manifest within this family? Are there phenotypic differences between the acquirable and chromosomally encoded MBLs? Moreover, what are the molecular properties that determine phenotypic variation? To date, there has been no study that systematically compares the MBLs and their diverse host organisms to address these questions. Understanding the genetic and molecular causes underlying phenotypic variation among MBLs is important in developing our ability to prevent and control the dissemination of multi-drug resistance genes.

Here, we conduct a comprehensive characterization of eight orthologous MBL enzymes to determine their resistance level in three bacterial hosts and unveil the extent to which genetic variation causes hidden phenotypic variation among them. We further performed diverse biochemical and biophysical characterizations of the enzymes to reveal the underlying molecular basis for the observed phenotypic variation.

Results

MBLs provide diverse levels of antibiotic resistance

We chose a set of eight MBLs to investigate the phenotypic variation in the B1-MBL family (Fig. 1 and Table 1): Three enzymes represent chromosomally encoded MBLs (BcII from *B. cereus*, IND-1 from *Chryseobacterium indologenes*, and CcrA from *Bacteroides fragilis*), and five represent those acquired on mobile genetic elements that have been identified in

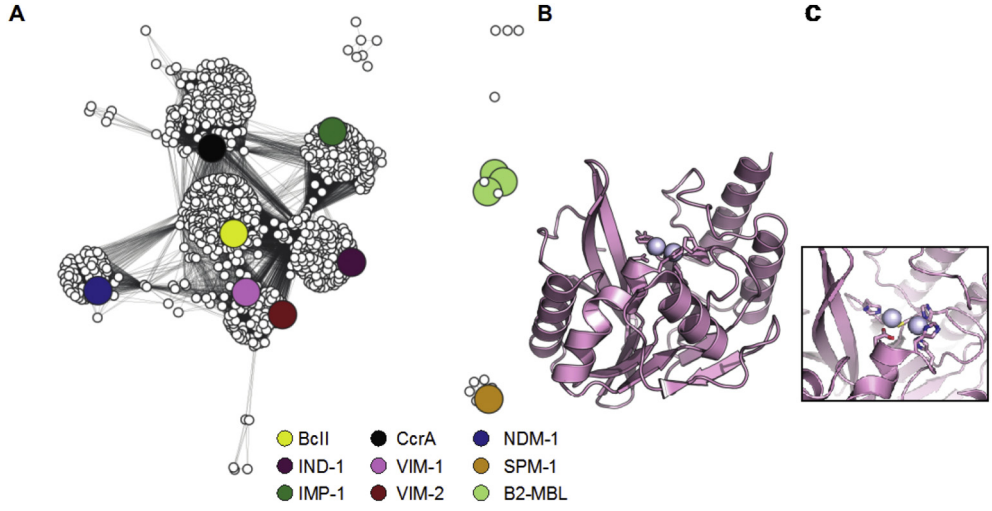

Fig. 1. Sequence similarity networks for the MBL family, with a representative crystal structure. (A) The sequence similarity network within the B1 and B2 MBL family with 1224 sequences visualized with a BLAST *e*-value cutoff of $1e^{-55}$. The sequences of the MBLs used in the study were shown as large circles and highlighted with colors: BcII (yellow), IND-1 (purple), CcrA (black), NDM-1 (blue), VIM-1 (pink), VIM-2 (red), IMP-1 (green), SPM-1 (orange), and the B2 MBL family (light green). Sequence identities between the MBLs are presented in Table 1 and Supplementary Table 1. (B) Cartoon presentation of the crystal structure of VIM-2 (PDB ID: 1K03). (C) The close-up view of the VIM-2 MBL active site that is conserved throughout the entire family: two zinc ions (shown as gray spheres) held in place by metal binding residues H-H-H and D-C-H (shown as sticks).

Table 1. Information of the eight MBLs that are used in this study

	Amino acid identity (%)								Mobility[a]	Common host organisms[b]	Accession number[c]
	BcII	IND-1	IMP-1	CcrA	VIM-1	VIM-2	NDM-1	SPM-1			
BcII	100								Chromosomal	*B. cereus*	AAA22276
IND-1	33	100							Chromosomal	*C. indologenes*	ABO21411
IMP-1	33	30	100						Acquired	*P. aeruginosa*, *A. baumanni*, *Serratia marcescens*, *E. cloacae*	AAN87168
CcrA	31	28	33	100					Chromosomal	*Bacillus fragilis*	AAA22904
VIM-1	36	27	30	29	100				Acquired	*P. aeruginosa*, *K. pneumoniae*, *S. marcescens*	CAE46717
VIM-2	36	25	32	28	90	100			Acquired	*E. coli*	AAK26253
NDM-1	28	23	31	29	35	34	100		Acquired	*E. coli*, *K. pneumoniae*, *E. cloacae*, *A. baumanni*	AFI72857
SPM-1	26	29	32	24	26	26	23	100	Acquired	*P. aeruginosa*	AAR15341

[a] Mobility indicates if the MBL is identified as a chromosomal copy in a single species of bacteria or the MBL has been transferred to multiple bacteria (acquired).
[b] Common host organisms indicate the original host of the MBL or the hosts that acquired the MBL and their closely related homologous (e.g., NDM-type). The information was obtained from Ref. [17].
[c] Accession number indicates National Center for Biotechnology Information (NCBI) accession no.

multiple bacterial pathogens (NDM-1, VIM-1, VIM-2, IMP-1, SPM-1). These enzymes also reflect the high sequence diversity within the B1-MBL family (amino acid identities between the enzymes range from 23% to 36%, except between VIM-1 and VIM-2, which is 90%) (Fig. 1, Table 1 and Supplementary Table 1). The MBL genes were subcloned into a modified broad-host-range pBBR1MCS-2 vector (5–10 plasmid copies per cell) [29,30] along with the inducible P_{BAD} promoter (pBBR1–pBAD) and subsequently transformed into three bacterial strains: *E. coli* E. cloni® *10G*, *P. aeruginosa* PA01, and *K. pneumoniae* ATCC13883. These three organisms were chosen because they represent major opportunistic pathogens that have recently acquired MBLs through HGT. The minimum inhibitory concentration (MIC) for the strains harboring the MBL genes was determined for six different compounds representing the three major classes of β-lactam antibiotics: cephalosporins (cefotaxime, and ceftazidime), carbapenems (meropenem, and imipenem) and penams (ampicillin, and penicillin). The bacterial growth was measured on agar plates supplemented with each antibiotic (the range of concentrations screened for each antibiotic was as follows: cephalosporins, 0.032 to 4096 μg/mL; carbapenems, 0.016 to 64 μg/mL; penams, 2 to 32768 μg/mL). It should be noted that the endogenous MIC of each strain for each antibiotic varies considerably due to their intrinsic resistance. Thus, we focused on quantifying the contribution of MBLs to increase MICs in each strain (Fig. 2).

The MBLs confer diverse levels of resistance (Fig. 2 and Supplementary Fig. 1, Supplementary Table 2). For example, there is an over 4000-fold range in the ceftazidime MIC between MBLs in *P. aeruginosa*, from 2 μg/mL for CcrA to 8192 μg/mL for NDM-1. Nonetheless, within each organism, the relative order of the MBLs by resistance was similar for the six different antibiotics. For example, IND-1 and VIM-1 in *E. coli* generally confer the highest MICs, followed by BcII, VIM-2, NDM-1, IMP-1, SPM-1, and lastly, CcrA. This indicates that the all MBLs exhibit similar broad substrate specificity, but the level of resistance that the enzymes confer varies significantly. By contrast, a different trend emerges when comparing the resistance levels across the three different organisms. For example, SPM-1, which confers one of the lowest MICs among the eight MBLs in *E. coli* (e.g., 32-fold lower ampicillin MIC than BcII, NDM-1, VIM-1, and IMP-1), provides a level of resistance equivalent to other MBLs such as BcII and NDM-1, and greater than IMP-1 in *P. aeruginosa*. CcrA, whose expression appears to be lethal in *E. coli* and thus did not result in formation of a colony even in the absence of antibiotics, is well tolerated in the other two organisms and even confers substantial resistance to *K. pneumoniae*. Taken together, these results suggest that the relationship between the MBL genes and their host organisms plays a strong role in determining the relative resistance that they provide.

Variation in enzyme catalytic efficiency fails to explain the variation in antibiotic resistance

The level of antibiotic resistance is generally considered to be strongly associated with the associate antibiotic resistance enzyme's catalytic efficiency (k_{cat}/K_M), and as a result, it is a common measurement that is made upon the discovery of a new MBL variants [31–33]. We examined to what extent the k_{cat}/K_M of the MBLs can explain the variation observed in their respective MICs. The mature MBL genes (with their signal peptides removed) were fused with a C-terminal strep-tag by subcloning into the pET-26(b) vector. The fusion proteins were subsequently overexpressed in *E. coli* BL21 (DE3) and purified, and their kinetic parameters (k_{cat}, K_M, and k_{cat}/K_M) were determined for the six β-

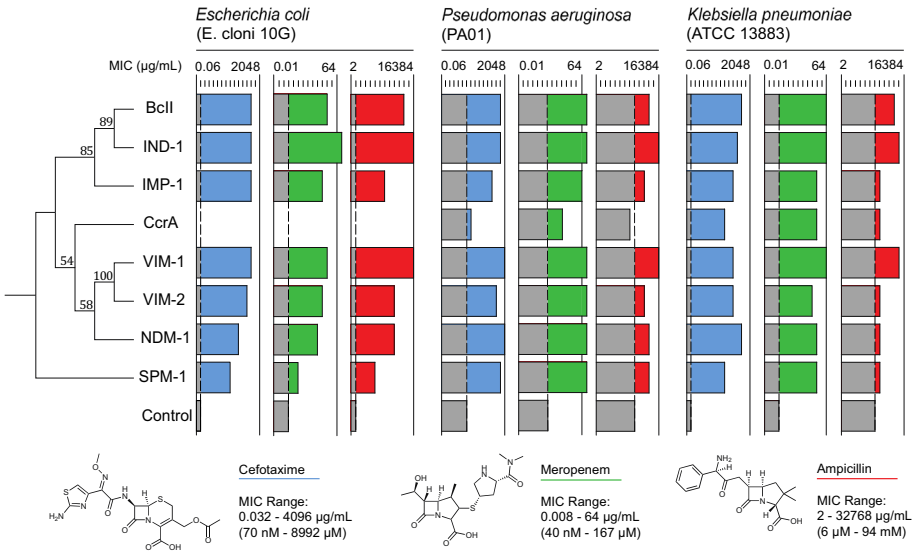

Fig. 2. Measured MICs for the MBLs with representative β-lactam antibiotics in *E. coli*, *P. aeruginosa*, and *K. pneumoniae*. MICs for cefotaxime (blue), meropenem (green), and ampicillin (red) measured for each MBL (BcII, IND-1, IMP-1, CcrA, VIM-1, VIM-2, NDM-1, and SPM-1) in *E. coli* 10G, *P. aeruginosa* PA01, and *K. pneumoniae* ATCC 13883. MICs were determined with the concentration at which at least three of four replicates did not grow. The gray bar represents the background resistance level of the organisms without MBL expression. The chemical structures of cefotaxime, meropenem, and ampicillin as well as the concentrations screened to determine the MICs are shown below. MICs for ceftazidime, imipenem, and penicillin are presented in Supplementary Fig. 1. The phylogenetic relationship of the orthologs is displayed in a maximum likelihood tree on the left, where the numbers represent bootstrap values of 500 replicates.

lactam substrates, in addition to a generic substrate, CENTA (Supplementary Fig. 2 and Supplementary Table 3). Overall, the eight MBLs are shown to be highly efficient enzymes for all seven substrates, with k_{cat}/K_M values ranging from 10^4 to 10^7 M^{-1} s^{-1}. For each substrate, the variation in k_{cat}/K_M between the MBLs is relatively small, with the difference between enzymes typically less than one order of magnitude (Supplementary Table 3). Interestingly, the relative enzyme catalytic efficiency of the MBLs rarely aligns with the level of resistance that the enzyme confers (Fig. 3 and Supplementary Fig. 3). Of the six antibiotics assessed with the three different organisms (18 combinations), the relationship between k_{cat}/K_M and MIC was generally uncorrelated in almost all cases. Only ceftazidime seems correlated in *E. coli* and *P. aeruginosa*. This is highlighted in *E. coli* in particular, where SPM-1 exhibits a 10-fold higher k_{cat}/K_M for ampicillin compared to VIM-2 (2.7×10^6 *versus* 2.7×10^5 M^{-1} s^{-1}), yet SPM-1 confers 256-fold lower resistance against ampicillin than VIM-2 (64 *versus* 16,384 μg/mL). While the existence of β-lactamase activity is essential to confer resistance to bacteria, the level of resistance that bacteria obtain cannot be explained by the kinetic parameters alone (k_{cat}/K_M). Hence, resistance must be strongly affected

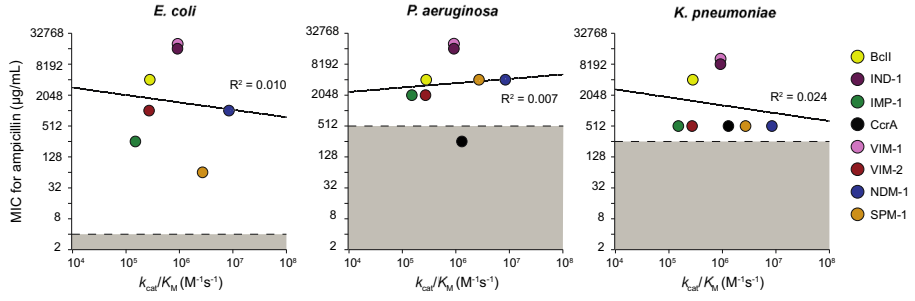

Fig. 3. Relationship between k_{cat}/K_M and ampicillin MICs for the MBLs in the three organisms. The measured ampicillin MIC values for each MBL in relation to their k_{cat}/K_M for each organism are shown. The background resistance for each organism is presented as the gray box. The relationship for the other five antibiotics is shown in Supplementary Fig. 3.

by other factors that are associated with the relationship between the host and the enzyme.

The combination of catalytic efficiency and periplasmic expression of MBLs determines the level of antibiotic resistance

The level of antibiotic resistance, or the fitness of the host strain (W), that is conferred by an MBL gene is the result of not only their catalytic efficiency (k_{cat}/K_M) but also abundance of functional enzyme in the periplasmic fraction of the cell ($[E_p]$). With a simplistic view, this relationship can be defined as $W \propto k_{cat}/K_M \times [E_p]$ [34,35]. To determine if this relationship can sufficiently explain the variation in observed resistance (MIC), we determined the $[E_p]$ of each enzyme by measuring the level of enzymatic activity in the periplasm fraction. Briefly, the cells that expressed MBLs were harvested, the periplasmic fractions were isolated using the osmotic shock method, and the level of β-lactamase activity in the periplasmic fraction was determined using 50 μM of CENTA. The number of functional MBL enzymes per cell in the periplasm fraction $[E_p]$ was then calculated using the kinetic parameters and the cell density of the cultures (see methods). It should be noted that two enzymes, NDM-1 and IND-1, showed very low activity in the periplasmic fraction, and thus, we omitted these enzymes from the following analyses. As a previous study demonstrated, NDM-1 is not a soluble periplasmic enzyme but rather localizes to outer membrane vesicles, and exhibits low concentrations in the periplasm despite consistently providing high levels of resistance [36,37]. IND-1 also exhibited unexpectedly low level of activities in the lysate enzymatic assay, and we speculate that IND-1 may be unstable in our assay buffer.

Of the six remaining MBLs, there was significant variation in the calculated $[E_p]$. The relative range in the variation of $[E_p]$ (over 1000-fold) was greater than that of k_{cat}/K_M (<100-fold) (Fig. 4A and Supplementary Fig. 4). For example, the $[E_p]$ of MBLs differs by more than >600-fold in *E. coli,* with SPM-1 expressing <20 molecules per cell and VIM-1 being produced >8000 molecules per cell. The relative order for the $[E_p]$ of six MBLs is similar across the three organisms (Supplementary Table 4); VIM-1 is consistently the most highly expressed enzyme with approximately 10-fold higher abundance than the other MBLs across all three organisms. By contrast, SPM-1 and CcrA are the lowest expressed enzymes in the three organisms. Nonetheless, the specific level of $[E_p]$ of each enzyme varies depending on the host organism (Supplementary Table 4). For example, VIM-2's periplasmic expression in *P. aeruginosa* is tripled compared to *E. coli*, whereas BcII's expression is halved. Therefore, the expression of each MBL enzyme is highly dependent on both its sequence and the host organism.

Overall, the variation in the antibiotic resistance levels conferred by MBLs is better explained using the equation, $\log(W) = \log(k_{cat}/K_M \times [E_p])$ (Fig. 4B and Supplementary Fig. 4), which captures the substantial

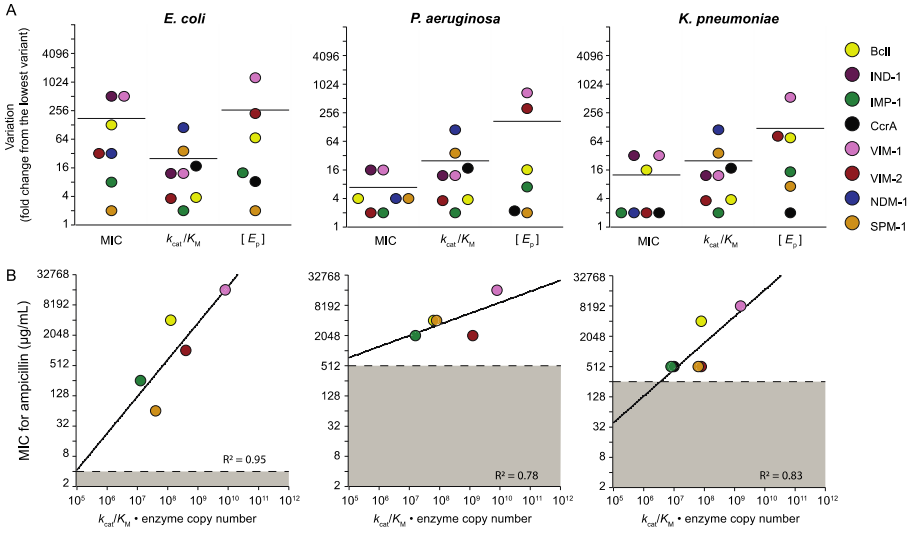

Fig. 4. Relationship between MIC, k_{cat}/K_M, and $[E_p]$ for each MBL in the three organisms. (A) The variation within MIC and the k_{cat}/K_M for ampicillin, and the $[E_p]$ (the protein expression level in the periplasm fraction) within each organism for the MBLs. Each data point represents the fold difference between the values for each MBL divided by the lowest value present for each property. The relationship for the other five antibiotics is shown in Supplementary Fig. 4. (B) The correlation between the product of k_{cat}/K_M and $[E_p]$ with MIC. NDM-1 and IND-1 were not included in the fit as NDM-1 is a known to be bound to the outer membrane and therefore could not be accurately measured with the assay, while IND-1 activity was not detectable in the assay. The relationship for the other five antibiotics is shown in Supplementary Fig. 5.

variation in k_{cat}/K_M and [E_p] for each enzyme in each organism. The results suggest that each MBL's MIC can be explained by variation in k_{cat}/K_M and [E_p]; however, it is noteworthy that MBL genetic variation appears to have a greater effect on expression rather than catalytic efficiency, suggesting that it is the dominant mechanism driving variation in conferred resistance.

The variation in MBL periplasmic expression reflects variation that emerges in multiple processes of protein expression

Next, we sought to understand the underlying molecular mechanisms that determine MBL periplasmic expression. We determined the extent of variation in each factor that is associated with the overall variation in enzyme expression in the periplasm, for example, the plasmid copy number, mRNA, and whole-cell enzyme expression, as well as the previously measured periplasmic protein concentration in *E. coli*. The variation between each MBL in plasmid copy-number and mRNA was measured by using quantitative PCR. The enzyme abundance in the cytoplasm fraction ([E_c]) was determined by lysing the spheroplasts (previously obtained during the periplasmic fraction isolation) and measuring the CENTA activity; the whole-cell enzyme abundance ([E_w]) is thus calculated by adding [E_c] and [E_p]. There is substantial variation in each molecule (DNA, RNA, and protein) among the eight MBLs (Fig. 5): The variation is presented as normalized numbers that is relative to the lowest variant for each assay. As expected, the variation in the amount of the plasmid copy number was relatively small (less than 3-fold difference). The small yet significant differences might stem from gene sequence of the MBLs that affect replication of the plasmids. However, variation in the level of mRNA is notably larger, exhibiting up to 16-fold difference between MBLs, indicating that the processivity and/or stability of mRNA differ depending on the MBL sequence. Moreover, the range of variation between the eight MBLs further increased after protein expression, from 210-fold at the whole cell protein level, to 650-fold in the periplasmic protein level (Fig. 5A). Interestingly, each enzyme behaves differently in each protein production process. For example, BcII exhibits the highest mRNA/DNA ratio, indicating that BcII mRNA is highly transcribed and/or stable in the cell (Fig. 5B–C). On the other hand, VIM-1 exhibits a high protein/mRNA ratio, suggesting that the high resistance of VIM1 is supported by high protein stability and/or translation rate (Fig. 5B–C). Moreover, the fraction of translocated enzymes (the ratio between periplasm and whole protein) varies significantly depending on the gene sequence: More than 30% of the VIM-1 and VIM-2 enzyme population were found in the periplasm, but SPM-1, IMP-1, and BcII present at less than 10% of proteins are translocated (Fig. 5D). This indicates that translocation is also a key factor in determining MIC.

Subsequently, in order to examine if the protein stability is correlated to the protein/mRNA ratio, we measured thermostability of the purified proteins. Interestingly however, we found that thermostability

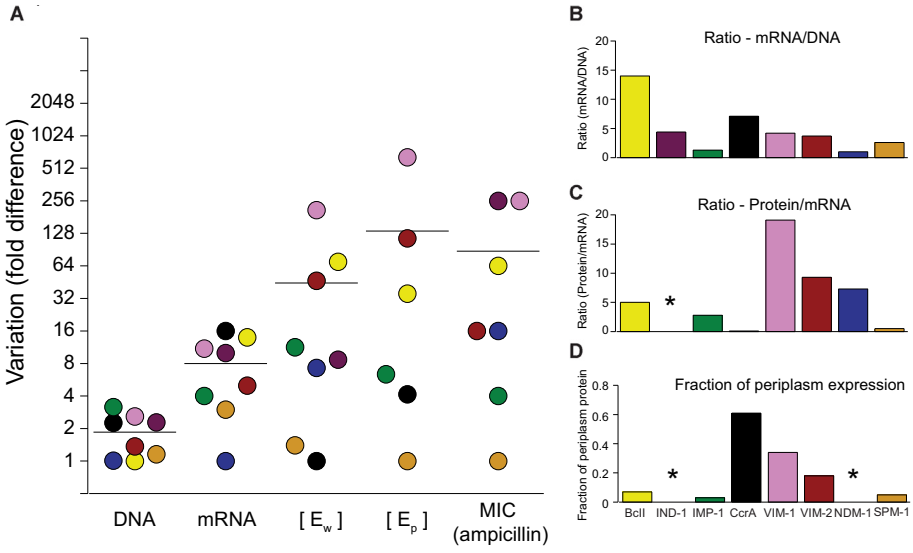

Fig. 5. The variation between MBLs at each level of expression compared to the variation in ampicillin resistance. (A) The variation within orthologs of various parameters normalized to the lowest value of each parameter. Parameters include the copy numbers of DNA (plasmids) and mRNA, the protein expression level in the whole cell [E_w] and in the periplasm fraction [E_w], and MIC. (B and D) The ratio between two parameters. Each data point represents the ratio of the fold difference between each MBL. (B) The ratio between mRNA and DNA. (C) The ration between [E_w] and mRNA. (C) The ratio between [E_p] and [E_w].

cannot explain variation in protein expression (Supplementary Fig. 5). For example, VIM-1, and VIM-2, and NDM-1 exhibit comparatively high levels of protein expression, but they show relatively moderate thermostability (<60 °C). SPM-1, by contrast, showed the highest thermostability (73 °C) despite exhibiting one of the lowest protein expression levels (Supplementary Fig. 5). This indicates that more the complicated properties of protein stability such as protein folding as well as translation processivity likely account for variation in protein expression [9,10,38,39]. Taken together, these results suggest that multiple properties such as mRNA, protein expression, stability, and translocation underlie the phenotypic variation across the MBLs.

A universal signal peptide does not fully abrogate phenotypic diversity

Establishing that translation and translocation are key factors in phenotypic variation, we sought to determine the effect of the signal peptide sequence on the MIC variation observed among MBLs. It has been demonstrated that the N-terminal region is strongly associated with the level of protein expression through its influence on translation initiation [40]. The N-terminal region also corresponds to the signal peptide of the translated protein, which would be expected to also exert significant influence on the efficacy of the MBL's translocation to the periplasm (or outer membrane for NDM-type MBLs) through its interactions with the signal recognition particle, trigger factor, or SecA, in addition to the SecYEG translocase [41,42]. This region also exhibits the highest level of genetic variation between the MBL genes, with no fully conserved residues and diverse lengths between 27 and 43 residues (as defined by where the first secondary structure element begins). Thus, we hypothesized that substitution of the native signal peptide of each MBL with a universal sequence may reduce the observed phenotypic variation.

The PelB leader sequence is a 22-amino-acid signal peptide sequence that was originally identified from the pectate lyase B gene from *Erwinia carotovora* and is extensively used for recombinant periplasmic protein expression in *E. coli* [43]. We replaced the native signal peptide of each MBL with the PelB sequence, generating PelB-MBL fusion genes in the pBBR1–pBAD vector, and determined the MICs of the three organisms harboring the constructs for the six β-lactam antibiotics (Supplementary Fig. 6). As predicted, the replacement of the signal peptide altered the MIC values; in some cases, the PelB peptide increased the MIC, for example, causing 8- and 2-fold increase for NDM-1 and SPM-1 in *E. coli* respectively. However, for other MBLs, the substitution of the native signal peptides with PelB either led to no change or a decrease in MIC (Fig. 6A). Consequently, the correlation between the PelB-MBL MICs and the measured catalytic efficiency became stronger compared to the MICs of the native MBLs (Fig. 6B and Supplementary Fig. 6). However, the correlations are still not as strong

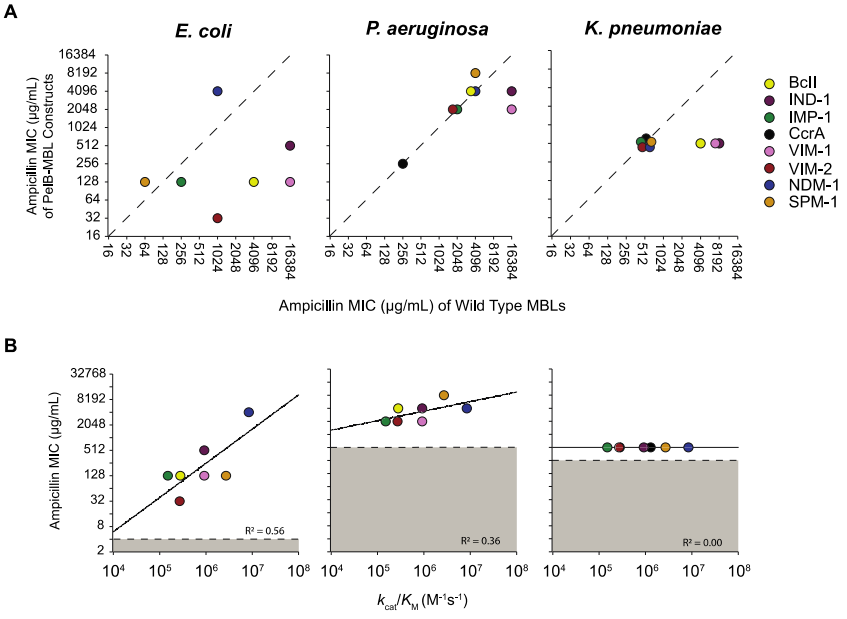

Fig. 6. The effects of the replacement of the native signal peptide with the PelB leader sequence on MBL-conferred resistance. (A) Relationship between the MICs for each MBL with their native signal peptide and with the PelB leader sequence for ampicillin, cefotaxime, and meropenem in *E. coli, P. aeruginosa,* and *K. pneumoniae*. (B) Correlation between the catalytic efficiency of each PelB-MBL (k_{cat}/K_M) and their ampicillin MICs. The relationships for the other five antibiotics are shown in Supplementary Fig. 7.

as those that take into account both catalytic efficiency and functional periplasmic expression. This suggests that while the sequences in the signal peptide region substantially contribute to the expression of the MBLs and thus the antibiotic resistance of the host organisms, the phenotypic variation observed among the family cannot by explained solely by the signal peptide sequences alone. Genetic variation throughout the entire gene plays a role in determining the level of functional periplasmic expression.

Discussion

With this work, we have systematically characterized eight B1-MBL enzymes and demonstrated that their genetic variation can cause substantial phenotypic variation upon expression in the same host organisms. Moreover, we observe strong variation not only for enzyme catalytic efficiency but also in terms of the each enzyme's functional periplasmic expression [44]. Enzyme functions are in general dictated by a subset of amino acid residues around the active site, while protein dynamics and long-range residual interactions also play roles for the function [45,46]. On the contrary, any mutation can contribute to changes in protein expression (e.g., protein and RNA stability, transcription, and translation rates) [47–51].

Our study holds important implications for the genetic compatibility of genes that are horizontally transferred to new host organisms and the relationship between sequence and gene expression. What are the molecular properties that determine protein expression and genetic compatibility? Many factors have been proposed to determine gene compatibility, such as GC content, codon usage, mRNA folding energy, and interactions to other proteins; however, the evidence from independent studies is often contradictory [11,40,52–57]. Indeed, our own attempts to investigate the effects of these proposed factors are also inconclusive. We measured the correlation of GC content and mRNA stability with relative mRNA expression levels in *E. coli*, and found that neither factor had a significant correlation with mRNA levels (Supplemental Fig. 8A–C, Supplemental Table 7). We also calculated the codon adaptation index (CAI) and tRNA adaptation index and found no significant correlation with whole-cell enzyme levels in all three hosts (Supplemental Fig. 8E–D, Supplemental Table 7). Finally, we also found that the fraction of rare codons contained within the orthologs did not correlate with enzyme levels in *E. coli* (Supplemental Fig. 8F, Supplemental Table 7). A recent study that assessed 200 diverse antibiotic resistance genes in *E. coli* demonstrated that many proposed factors mentioned above could not sufficiently explain the compatibility of the heterologous genes. Instead, only phylogenetic distance (i.e., evolutionary distance between the original and new hosts) and mechanistic compatibility with the host (i.e., dependency upon specific components of the host's physiology and metabolism) provided a generally accurate estimation of protein fitness [5]. Similarly, a study of human gut microbiota demonstrated that horizontal transfer of antimicrobial peptide resistance is constrained by phylogenetic barriers [58]. Other studies suggest that genes encoding for proteins involved in many interactions to other molecules in the cell are less prone to be subject to HGT than genes encoding for proteins that carry a single function [59,60]. Our observations suggest that variation in MBL fitness is caused by every step of the protein expression process, including transcription, translation, and translocation. Thus, it is unlikely that a single parameter can explain genetic compatibility and protein expression in the cell, and it is essential to develop comprehensive models with multiple parameters to understand genetic incompatibility.

Another important finding is the observation that translocation is one of the mechanisms for genetic incompatibility. To date, a general trend in the signal peptide sequence has been identified for each translocation system (e.g., the Sec protein translocation pathway) [61–65]. However, we have little understanding of the relationship between the signal peptide sequence and its translocation efficacy, let alone the incompatibility between the translocation system of a particular organism and the signal peptide sequence of a particular gene. Indeed, the signal peptide is the most variable region in the MBL sequence. While many changes in the signal peptide sequence are likely due to “neutral” genetic drift, some may be associated with co-evolution with the host translocation system. Developing our understanding of the universal rules for the relationship between signal peptide sequences and protein translocation should be a priority if we are to better understand the molecular basis of HGT and genetic incompatibility.

HGT is the primary mechanism underlying the dissemination of antibiotic resistance genes to different bacterial hosts [12,58]. Needless to say, the host compatibility of associated genetic elements such as the transcription and translation initiation sequences and the origin of replication (in the case of the plasmids) have a significant impact on the outcome of HGT. However, our results suggest that coding region can itself play a significant role in a gene's dissemination [66,67]. It has been shown that acquired MBLs exhibit some bias with respect to the bacterial hosts that harbor them. For example, SPM-type MBLs have been noted for their strong association with *P. aeruginosa* [68], whereas NDM-type MBLs are predominantly found in *K. pneumoniae* and *E. coli* (Table 1) [69]. Our study's results are broadly consistent with these clinical observations, that is, SPM-1 confers relatively high resistance in *P. aeruginosa*, but much lower resistance in *E. coli* and *K. pneumonia.* Moreover, a chromosomally encoded

MBL, CcrA from *Bacteroides fragilis* appears to be toxic when expressed in *E. coli* and *P. aeruginosa* despite conferring substantial resistance in *K. pneumoniae*. Beyond such examples, however, we did not observe any particular trend that differentiates acquirable MBLs from non-mobile MBLs. A more comprehensive survey using diverse clinical strains and the integration with other functional genetic elements, such as the native ribosome-binding site and promoter, may be needed to detect a more pronounced tendency [70]. In addition, there may be other specific features of MBLs that could be associated with high antibiotic resistance of pathogens in the human body. For example, recent studies demonstrated that NDM-1 variants possess the unique quality of being active in a partially zinc-depleted environment [71].

Lastly, our observations emphasize the importance of establishing comprehensive methodologies and protocols when studying newly isolated antibiotic resistance genes and variants. Antibiotic resistance variants continue to be isolated in clinical environments in increasing numbers, and in general, there has been more emphasis placed on determining their kinetic parameters, with less concern paid to the detectable protein expression [72]. We suggest that more effort is warranted for developing universal procedures and protocols. For example, the use of a universal expression vector for multiple-host expression ability and representative clinically related model bacterial hosts to assess MBL variants *in situ* would allow for a more complete assessment of new clinical threats and facilitate the identification of hidden molecular properties that may be causing higher antibiotic resistance.

Methods and Materials

Construction of sequence similarity networks

A representative sequence similarity network [73,74] for the MBL B1 family was created by performing a protein BLAST on VIM-2 and then downloading all sequences with *e*-values of $10e^{-15}$ and lower on March 23, 2017. This cutoff was enough to include the adjacent B2 family seen in the full representative network, but limited other members of the superfamily. The sequences were filtered by length using the Galaxy Bioinformatics Suite (175 to 425 amino acids) before culling duplicate sequences with CD-HIT by using an identity threshold of 100%. The remaining 1199 sequences were added to 25 representative B1 and B2 MBL sequences (CphA, ImiS, Sfh-1, BlaB, EBR-1, SFB-1, SLB-1, GIM-1, SIM-1, KHM-1, DIM-1, PEDO-3, MUS-1, MUS-2, JOHN-1, CGB-1, TUS-1, BcII, CcrA, IND-1, NDM-1, VIM-1, VIM-2, IMP-1, and SPM-1) before an all *versus* all protein BLAST (National Center for Biotechnology Information, version 2.2.28+) with a threshold cutoff of $10e^{-55}$. The network was visualized with an organic layout in Cytoscape.

Cloning and expression of MBLs in *E. coli*, *P. aeruginosa*, and *K. pneumoniae*

The eight MBL genes were synthesized (BioBasic) and subcloned in a broad-host-range vector, pBBR1MCS-2, along with the P_{BAD} promoter, which is inducible in the presence of arabinose (5.9-vector). The plasmids were transformed into three bacterial strains: *E. coli 10G* (chemical transformation), *P. aeruginosa* PA01 (electroporation) [75], and *K. pneumoniae* ATCC13883 (electroporation) [76].

Determination of MIC values

To determine the MIC for each β-lactam antibiotic, single colonies of *E. coli* 10G, *P. aeruginosa* PA01, and *K. pneumoniae* ATCC 13883 that were transformed with the MBL plasmids were picked and grown in quadruplicate overnight at 30 °C in a 96-well plate in 500 μL of LB media with 1% glucose to suppress expression and 40 μg/mL of kanamycin for selective resistance. The overnight culture was used at a 1:40 dilution to start a new 200-μL culture of LB media supplemented with 40 μg/mL of kanamycin and 0.02% arabinose to induce expression. The cells were grown for 6 h at 37 °C before being transferred with replicator pins onto a series of LB agar plates containing two-fold increases in the concentration of antibiotic and 0.02% arabinose and grown overnight at 37 °C (the range of concentrations screened for each antibiotic was as follows: cephalosporins, 0.032 to 4096 μg/mL; carbapenams, 0.016 to 64 μg/mL; penams, 2 to 32,768 μg/mL). The MICs were determined at the concentration of antibiotics by which no growth was observed at least three of the four replicates.

Purification of Strep-tagged MBLs

All MBL variants were cloned into a pET-26(b) vector without their signal peptide and with a C-terminal Strep-tag (GNSGSAWSHPQFEK). Each enzyme was expressed in *E. coli* BL21 (DE3) cells in TB auto-induction media (EMD Millipore) supplemented with 1% (w/v) glycerol, 200 μM $ZnCl_2$, and 40 μg/mL kanamycin. Cultures (200 mL) were inoculated with 5 mL of overnight culture (LB media, 40 μg/mL of kanamycin) and incubated at 30 °C for 6 h before further incubation at 18 °C for 10 h. Cells were harvested by centrifugation at 3200*g* and pellets were frozen at −80 °C overnight. Cell pellets were resuspended in the lysis buffer containing 50% B-PER protein extraction reagent (Thermo Scientific) in buffer A [50 mM Tris–HCl (pH 7.5), 100 mM NaCl, and 200 μM $ZnCl_2$] and 100 μg/mL of lysozyme, and incubated on ice for

1 h. The cell lysates were centrifuged at 25,000*g* for 30 min at 4 °C and the Strep-tag fusion proteins were purified from the clarified lysate according to the manufacturer's instruction with Strep-tactin resin (IBA Lifesciences). The purified protein solution was desalted using Econo-Pac 10DG Column (Bio-Rad) and eluted in 4 mL of buffer H [20 mM Hepes (pH 7.5), 100 mM $NaCl_2$, 200 μM $ZnCl_2$]. The concentration of each protein was determined by spectrophotometer. The A_{280} was measured for each sample with the following extinction coefficients: BcII, 34,950 M^{-1} cm^{-1}; IND-1, 40,910 M^{-1} cm^{-1}; IMP-1, 50,420 M^{-1} cm^{-1}; CcrA, 46,410 M^{-1} cm^{-1}; VIM-1, 33,920 M^{-1} cm^{-1}; VIM-2, 35,410 M^{-1} cm^{-1}; NDM-1, 33,460; SPM-1, 36,440 M^{-1} cm^{-1}.

Enzyme assays to determine kinetic parameters

The catalytic ability of each MBL enzyme was measured for seven β-lactam substrates (CENTA, cefotaxime, ceftazidime, meropenem, imipenem, ampicillin, and benzylpenicillin) in buffer H supplemented with 0.2% Triton X-100. The rate of hydrolysis of CENTA was determined by measuring changes in the absorbance at 405 nm (the extinction coefficient of CENTA at 405 nm is 6400 M^{-1} cm^{-1}). The rate of hydrolysis of the β-lactam ring in the six antibiotics was determined by measuring decrease in absorbance at the following wavelengths with these reported extinction coefficients: cefotaxime, 260 nm, 7500 M^{-1} cm^{-1}; ceftazidime, 260 nm, 9000 M^{-1} cm^{-1}; meropenem, 300 nm, 6500 M^{-1} cm^{-1}; imipenem, 300 nm, 9000 M^{-1} cm^{-1}; ampicillin 235 nm, 820 M^{-1} cm^{-1}; and benzylpenicillin, 235 nm, 775 M^{-1} cm^{-1}. The initial rates of reaction were measured in triplicate over the range of substrate concentrations (1 to 400 μM for CENTA, cefotaxime, ceftazidime, meropenem, and imipenem, and 25 to 2000 μM for ampicillin and benzylpenicillin). The rates were used to determine the kinetic constants for each enzyme–substrate pair by fitting the data with the Michaelis–Menten equation using KaleidaGraph (Synergy). For those pairs where substrate saturation of the enzyme was not possible, the linear portion of the Michaelis–Menten plot was used to determine the k_{cat}/K_M values.

Cellular fractionation and the β-lactamase activity measurement in the cell lysate

To quantify the expression of the MBLs in the periplasm, cytoplasm, and whole-cell fractions, single colonies from *E. coli* 10G, *P. aeruginosa* PA01, and *K. pneumoniae* ATCC 13883 transformed with the MBL plasmids were picked, grown in quadruplicate overnight at 30 °C in a 96-well plate in 200 μL of LB media with 1% glucose to suppress expression and 40 μg/mL of kanamycin for selective resistance. A 1:40 dilution was used to start a 500-μL LB media expression culture that was grown for 6 h at 37 °C with 0.02% arabinose for induction and 40 μg/mL of kanamycin. The cells were collected by centrifugation at 3200*g* for 10 min. The periplasmic fractions were isolated using the osmotic shock protocol. The pellets were suspended in OS1 buffer [30 mM Tris–HCl (pH 7.1), 20% sucrose, and 1 mM phenylmethylsulfonyl fluoride] and incubated for 30 min at room temperature before centrifugation (3200*g* for 10 min). The pellets were then resuspended in OS2A buffer (ice-cold 0.5 mM $MgCl_2$) and incubated on ice for 5 min before centrifugation (3200*g* for 10 min). One hundred microliters of the supernatant was collected and mixed with 100 μL OS2B [40 mM Hepes (pH 7.5), 200 mM NaCl, 400 μM $ZnCl_2$, and 0.4% Triton]. The initial rate of β-lactamase activity was measured by mixing the isolated periplasm fraction and 50 μM of CENTA at a 1:10 ratio in buffer H supplemented with 0.2% Triton X-100. The remaining pellets were then frozen overnight at −20 °C. To obtain the cytoplasmic fraction, the frozen pellets were resuspended in 200 μL of lysis buffer [20 mM Hepes (pH 7.5), 100 mM NaCl, 200 μM $ZnCl_2$, 0.2% Triton, 200 μg/mL lysozyme, 1 U benzonase (Millipore), and 0.25 mM $MgCl_2$] and incubated at room temperature for 1 h. After centrifugation (3200*g* for 10 min), the supernatant was removed and β-lactamase activity was measured to determine the level of enzymes in the cytoplasm.

Calculation of the number of functional MBLs per fraction

The initial rate of reaction with CENTA for the fractional or whole-cell lysates was used in conjunction with the initial rate measured with purified enzyme to determine the relative amount of enzyme in each fraction: $[E] = ((A_{lysate} \div A_{purified}) \times [E_{purified}] \times V \times N_A) \div (OD_{600} \times 1 \times 10^9\ CFU/OD_{600})$, where A_{lysate} denotes the rate of CENTA hydrolysis in the lysate, $A_{purified}$ denotes the rate of CENTA hydrolysis of purified enzyme, $[E_{purified}]$ denotes the concentration of purified enzyme, V denotes the culture volume, N_A denotes Avogadro's constant, and OD_{600} denotes the absorbance of the cultures at 600 nm.

Determination of MBL gene expression

After induction of the *E. coli* harboring each MBL as described above, plasmid DNA was isolated from 500 μL of culture with a QIAprep Miniprep Kit (Qiagen). For isolation of RNA, 500 μL of the induced culture was mixed with 500 μL of RNAprotect Bacteria Reagent (Qiagen) and incubated at room temperature for 5 min before RNA extraction as per the manufacturer's instructions with the RNeasy Mini Kit (Qiagen). To ensure removal of contaminating DNA, the samples were processed with a DNA-Free kit (Ambion). cDNA

was then prepared using the QuantiTect Reverse Transcription Kit (Qiagen).

Quantitative PCR was performed on a 7500 Fast Real-Time PCR System (Applied Biosystems) with the following cycling conditions: 20 s at 95 °C, followed by 40 cycles of 95 °C for 3 s and 58 °C for 30 s. The primers used for the DNA quantification were designed to detect the pBBR1–pBAD vector: F-CCAA CAGCGATTCGTCCTGG, R-AGCCAGAAGACA CTTTCCAAGC. The forward primers used for the RNA quantification were designed for each MBL: BcII, F-GATTTAGGAAACGTTGCGGATGC; IND-1, F-CAATGTATTGGATGGTGGCTGTC; CcrA, F-GCAT GGCCGAAAACTCTCG; NDM-1, F-CTCGGCAATC TCGGTGATGC; VIM-1, F-GGAAGCAGAGGTCGTC ATTCC; VIM-2, F-GGAAGCACAGTTCGTCATTCC; IMP-1, F-TAGAAGCTTGGCCAAAGTCCG; and SPM-1, F-AACTTGGTTATCTGGGAGATGCC. The reverse primer was the same for all eight MBLs: R-GCAACGCAATTAATGTGAGTTAGC. The primers for the reference gene, histidyl-RNA synthetase (*hisS*), were: F-GCTCCGGCATTAGGTGATTA and R-TCAAGCAGTTTGCACAGACC. Normalized expression units for each MBL gene were calculated using the ΔΔCt method relative to *hisS*, whereas the absolute value of the number of DNA copy number was determined with known standards of the vector, pBBR1–pBAD, and normalized by the OD_{600} of the original culture.

Replacement of MBL signal peptides with the PelB leader sequence

The native signal peptides for each MBL were replaced in the pBBR1–pBAD vector with the PelB leader sequence (MGKYLLPTAAAGLLLLAAQPA-MAMDSG) using Golden Gate assembly cloning with the Type IIS restriction enzyme, BsaI.

Calculation of RNA stability and codon optimality

RNA folding free energy for all orthologs was estimated using two web-based prediction tools, NUPACK [77] and DINAMelt zip fold [78]. Default RNA options were used for NUPACK, while the RNA 3.0 option of zipfold was used for DINAMelt. GC content was calculated in-house using a python script. The tRNA adaptation index was calculated for *E. coli* and *P. aeruginosa* using the web-based tool stAIcalc [79]. The CAI of all three hosts was calculated in-house using the method by Sharp and Li [80], where the 27 *E. coli* genes [81] and their orthologs in the other hosts were collected from NCBI for the calculation of CAI (Supplemental Table 8). The fraction of eight rare codons excluded from highly expressed genes [82] contained within each of the ortholog genes was calculated using an in-house Python script.

CRediT authorship contribution statement

Raymond D. Socha: Conceptualization, Formal analysis, Investigation, Writing - original draft. **John Chen:** Formal analysis, Writing - review & editing. **Nobuhiko Tokuriki:** Conceptualization, Formal analysis, Supervision, Funding acquisition, Writing - original draft, Writing - review & editing.

Acknowledgments

We thank the members of the Tokuriki laboratory for comments on the manuscript. A Canadian Institute of Health Research (CIHR) foundation grant (353714) was provided to N.T. N.T. is a CIHR new investigator and a Michael Smith Foundation of Health Research (MSFHR) career investigator.

Author Contributions: R.D.S. and N.T. conceived and designed this study. R.D.S. performed experiments. J.C. performed computational analyses of gene sequences. R.D.S. and N.T. wrote the paper.

Appendix A. Supplementary data

Supplementary data to this article can be found online at https://doi.org/10.1016/j.jmb.2019.01.041.

Received 5 October 2018;
Received in revised form 31 January 2019;
Accepted 31 January 2019
Available online 13 February 2019

Keywords
Phenotypic variation;
Metallo-beta-lactamase;
Genetic incompatibility;
Protein expression;
Horizontal gene transfer

Abbreviations used:
HGT, horizontal gene transfer; MBL, metallo-β-lactamase; MIC, minimum inhibitory concentration; CAI, codon adaptation index.

References

[1] M. Kimura, Evolutionary rate at the molecular level, Nature 217 (1968) 624–626.
[2] B. Charlesworth, D. Charlesworth, Neutral variation in the context of selection, Mol. Biol. Evol. 35 (2018) 1359–1361, https://doi.org/10.1093/molbev/msy062.

[3] S.C. Lovell, D.L. Robertson, An integrated view of molecular coevolution in protein-protein interactions, Mol. Biol. Evol. 27 (2010) 2567–2575, https://doi.org/10.1093/molbev/msq144.
[4] S.M. Soucy, J. Huang, J.P. Gogarten, Horizontal gene transfer: building the web of life, Nat. Rev. Genet. 16 (2015) 472–482, https://doi.org/10.1038/nrg3962.
[5] A. Porse, T.S. Schou, C. Munck, M.M.H. Ellabaan, M.O.A. Sommer, Biochemical mechanisms determine the functional compatibility of heterologous genes, Nat. Commun. 9 (2018) 522, https://doi.org/10.1038/s41467-018-02944-3.
[6] S. Bhattacharyya, M. Manhart, E.I. Shakhnovich, Protein homeostasis imposes a barrier on functional integration of horizontally transferred genes in bacteria, PLoS Genet. 11 (2015) e1005612, https://doi.org/10.1371/journal.pgen.1005612.
[7] A.B. Paaby, M.V. Rockman, Cryptic genetic variation: evolution's hidden substrate, Nat. Rev. Genet. 15 (2014) 247–258, https://doi.org/10.1038/nrg3688.
[8] S. Schlegel, E. Rujas, A.J. Ytterberg, R.A. Zubarev, J. Luirink, J.-W. de Gier, Optimizing heterologous protein production in the periplasm of *E. coli* by regulating gene expression levels, Microb. Cell Factories 12 (2013) 24, https://doi.org/10.1186/1475-2859-12-24.
[9] S. Bershtein, W. Mu, A.W.R. Serohijos, J. Zhou, Protein quality control acts on folding intermediates to shape the effects of mutations on organismal fitness, Mol. Cell 49 (2013) 133–144, https://doi.org/10.1016/j.molcel.2012.11.004.
[10] S. Bershtein, W. Mu, E.I. Shakhnovich, Soluble oligomerization provides a beneficial fitness effect on destabilizing mutations, Proc. Natl. Acad. Sci. U. S. A. 109 (2012) 4857–4862, https://doi.org/10.1073/pnas.1118157109.
[11] S. Bhattacharyya, J. Yan, E.I. Shakhnovich, Transient protein-protein interactions perturb *E. coli* metabolome and cause gene dosage toxicity, eLife 5 (2016) 103, https://doi.org/10.7554/eLife.20309.
[12] C.J.H. von Wintersdorff, J. Penders, J.M. van Niekerk, N.D. Mills, S. Majumder, L.B. van Alphen, et al., Dissemination of antimicrobial resistance in microbial ecosystems through horizontal gene transfer, Front. Microbiol. 7 (2016) 173, https://doi.org/10.3389/fmicb.2016.00173.
[13] H.C. Maltezou, Metallo-beta-lactamases in gram-negative bacteria: introducing the era of pan-resistance? Int. J. Antimicrob. Agents 33 (2009) 405.e1-7, https://doi.org/10.1016/j.ijantimicag.2008.09.003.
[14] G. Cornaglia, H. Giamarellou, G.M. Rossolini, Metallo-β-lactamases: a last frontier for β-lactams? Lancet Infect. Dis. 11 (2011) 381–393, https://doi.org/10.1016/S1473-3099(11)70056-1.
[15] A.U. Khan, L. Maryam, R. Zarrilli, Structure, genetics and worldwide spread of New Delhi metallo-β-lactamase (NDM): a threat to public health, BMC Microbiol. 17 (2017) 101, https://doi.org/10.1186/s12866-017-1012-8.
[16] P. Nordmann, L. Poirel, T.R. Walsh, D.M. Livermore, The emerging NDM carbapenemases, Trends Microbiol. 19 (2011) 588–595, https://doi.org/10.1016/j.tim.2011.09.005.
[17] A.G. McArthur, N. Waglechner, F. Nizam, A. Yan, M.A. Azad, A.J. Baylay, et al., The comprehensive antibiotic resistance database, Antimicrob. Agents Chemother. 57 (2013) 3348–3357, https://doi.org/10.1128/AAC.00419-13.
[18] Metallo-β-lactamase structure and function, Ann. N. Y. Acad. Sci. 1277 (2013) 91–104, https://doi.org/10.1111/j.1749-6632.2012.06796.x.
[19] C. Bebrone, Metallo-β-lactamases (classification, activity, genetic organization, structure, zinc coordination) and their superfamily, Biochem. Pharmacol. 74 (2007) 1686–1701, https://doi.org/10.1016/j.bcp.2007.05.021.
[20] F. Baier, N. Tokuriki, Connectivity between catalytic landscapes of the metallo-β-lactamase superfamily, J. Mol. Biol. 426 (2014) 2442–2456, https://doi.org/10.1016/j.jmb.2014.04.013.
[21] G.J. Cuchural, M.H. Malamy, F.P. Tally, Beta-lactamase-mediated imipenem resistance in *Bacteroides fragilis*, Antimicrob. Agents Chemother. 30 (1986) 645–648.
[22] S. Bellais, S. Léotard, L. Poirel, T. Naas, P. Nordmann, Molecular characterization of a carbapenem-hydrolyzing beta-lactamase from *Chryseobacterium* (*Flavobacterium*) *indologenes*, FEMS Microbiol. Lett. 171 (1999) 127–132.
[23] E. Osano, Y. Arakawa, R. Wacharotayankun, M. Ohta, T. Horii, H. Ito, et al., Molecular characterization of an enterobacterial metallo beta-lactamase found in a clinical isolate of *Serratia marcescens* that shows imipenem resistance, Antimicrob. Agents Chemother. 38 (1994) 71–78.
[24] L. Poirel, C. Héritier, P. Nordmann, Genetic and biochemical characterization of the chromosome-encoded class B beta-lactamases from *Shewanella livingstonensis* (SLB-1) and *Shewanella frigidimarina* (SFB-1), J. Antimicrob. Chemother. 55 (2005) 680–685, https://doi.org/10.1093/jac/dki065.
[25] S. Bellais, D. Girlich, A. Karim, P. Nordmann, EBR-1, a novel ambler subclass B1 beta-lactamase from *Empedobacter brevis*, Antimicrob. Agents Chemother. 46 (2002) 3223–3227, https://doi.org/10.1128/AAC.46.10.3223-3227.2002.
[26] T.R. Walsh, M.A. Toleman, L. Poirel, P. Nordmann, Metallo-beta-lactamases: the quiet before the storm? Clin. Microbiol. Rev. 18 (2005) 306–325, https://doi.org/10.1128/CMR.18.2.306-325.2005.
[27] B. Jia, A.R. Raphenya, B. Alcock, N. Waglechner, P. Guo, K. K. Tsang, et al., CARD 2017: expansion and model-centric curation of the comprehensive antibiotic resistance database, Nucleic Acids Res 45 (2017) D566–D573, https://doi.org/10.1093/nar/gkw1004.
[28] M. Widmann, J. Pleiss, P. Oelschlaeger, Systematic analysis of Metallo-β-lactamases using an automated database, Antimicrob. Agents Chemother. 56 (2012) 3481–3491, https://doi.org/10.1128/AAC.00255-12.
[29] M.E. Kovach, P.H. Elzer, D.S. Hill, G.T. Robertson, M.A. Farris, R.M. Roop, et al., Four new derivatives of the broad-host-range cloning vector pBBR1MCS, carrying different antibiotic-resistance cassettes, Gene 166 (1995) 175–176.
[30] S.R. Khan, J. Gaines, R.M. Roop, S.K. Farrand, Broad-host-range expression vectors with tightly regulated promoters and their use to examine the influence of TraR and TraM expression on Ti plasmid quorum sensing, Appl. Environ. Microbiol. 74 (2008) 5053–5062, https://doi.org/10.1128/AEM.01098-08.
[31] Z. Liu, J. Li, X. Wang, D. Liu, Y. Ke, Y. Wang, et al., Novel variant of New Delhi metallo-β-lactamase, NDM-20, in *Escherichia coli*, Front. Microbiol. 9 (2018) 248, https://doi.org/10.3389/fmicb.2018.00248.
[32] C.C. Papagiannitsis, S. Pollini, G.M. Rossolini, J.-D. Docquier, Biochemical characterization of VIM-39, a VIM-1-like metallo-β-lactamase variant from a multidrug-resistant *Klebsiella pneumoniae* isolate from Greece, Antimicrob. Agents Chemother. 59 (2015) 7811–7814, https://doi.org/10.1128/AAC.01935-15.
[33] K. Jeannot, L. Poirel, M. Robert-Nicoud, P. Cholley, P. Nordmann, P. Plésiat, IMP-29, a novel IMP-type metallo-β-

lactamase in *Pseudomonas aeruginosa*, Antimicrob. Agents Chemother. 56 (2012) 2187–2190, https://doi.org/10.1128/AAC.05838-11.
[34] N. Tokuriki, D.S. Tawfik, Stability effects of mutations and protein evolvability, Curr. Opin. Struct. Biol. 19 (2009) 596–604, https://doi.org/10.1016/j.sbi.2009.08.003.
[35] M. Kaltenbach, Dynamics and constraints of enzyme evolution, J. Exp. Zool. B Mol. Dev. Evol. 322 (2014) 468–487, https://doi.org/10.1002/jez.b.22562.
[36] D. King, N. Strynadka, Crystal structure of New Delhi metallo-β-lactamase reveals molecular basis for antibiotic resistance, Protein Sci. 20 (2011) 1484–1491, https://doi.org/10.1002/pro.697.
[37] L.J. González, G. Bahr, T.G. Nakashige, E.M. Nolan, A.J. Vila, Membrane anchoring stabilizes and favors secretion of New Delhi metallo-β-lactamase, Nat. Chem. Biol. 12 (2016) 516–522, https://doi.org/10.1038/nchembio.2083.
[38] K.T. Wyganowski, M. Kaltenbach, N. Tokuriki, GroEL/ES buffering and compensatory mutations promote protein evolution by stabilizing folding intermediates, J. Mol. Biol. 425 (2013) 3403–3414, https://doi.org/10.1016/j.jmb.2013.06.028.
[39] S.A. Lim, K.M. Hart, K.M. Hart, M.J. Harms, S. Marqusee, Evolutionary trend toward kinetic stability in the folding trajectory of RNases H, Proc. Natl. Acad. Sci. U. S. A. 113 (2016) 13045–13050, https://doi.org/10.1073/pnas.1611781113.
[40] G. Kudla, A.W. Murray, D. Tollervey, J.B. Plotkin, Coding-sequence determinants of gene expression in *Escherichia coli*, Science. 324 (2009) 255–258, https://doi.org/10.1126/science.1170160.
[41] A. Tsirigotaki, J. De Geyter, N. Šoštaric, A. Economou, S. Karamanou, Protein export through the bacterial Sec pathway, Nat. Rev. Microbiol. 15 (2017) 21–36, https://doi.org/10.1038/nrmicro.2016.161.
[42] J.M. Crane, The sec system: protein export in *Escherichia coli*, EcoSal Plus 7 (2017)https://doi.org/10.1128/ecosalplus.ESP-0002-2017.
[43] B.E. Power, N. Ivancic, V.R. Harley, R.G. Webster, A.A. Kortt, R.A. Irving, et al., High-level temperature-induced synthesis of an antibody VH-domain in *Escherichia coli* using the PelB secretion signal, Gene 113 (1992) 95–99.
[44] R.D. Socha, N. Tokuriki, Modulating protein stability-directed evolution strategies for improved protein function, FEBS J. 280 (2013) 5582–5595, https://doi.org/10.1111/febs.12354.
[45] K.L. Morley, R.J. Kazlauskas, Improving enzyme properties: when are closer mutations better? Trends Biotechnol. 23 (2005) 231–237, https://doi.org/10.1016/j.tibtech.2005.03.005.
[46] C.M. Miton, N. Tokuriki, How mutational epistasis impairs predictability in protein evolution and design, Protein Sci. 25 (2016) 1260–1272, https://doi.org/10.1002/pro.2876.
[47] N. Tokuriki, F. Stricher, J. Schymkowitz, L. Serrano, D.S. Tawfik, The stability effects of protein mutations appear to be universally distributed, J. Mol. Biol. 369 (2007) 1318–1332, https://doi.org/10.1016/j.jmb.2007.03.069.
[48] J.R. Klesmith, J.-P. Bacik, E.E. Wrenbeck, R. Michalczyk, T. A. Whitehead, Trade-offs between enzyme fitness and solubility illuminated by deep mutational scanning, Proc. Natl. Acad. Sci. U. S. A. 114 (2017) 2265–2270, https://doi.org/10.1073/pnas.1614437114.
[49] E. Firnberg, E. Firnberg, J.W. Labonte, J.W. Labonte, J.J. Gray, J.J. Gray, et al., A comprehensive, high-resolution map of a gene's fitness landscape, Mol. Biol. Evol. 31 (2014) 1581–1592, https://doi.org/10.1093/molbev/msu081.
[50] A. Delgado, R. Arco, B. Ibarra-Molero, J.M. Sanchez-Ruiz, Using resurrected ancestral proviral proteins to engineer virus resistance, Cell Rep. 19 (2017) 1247–1256, https://doi.org/10.1016/j.celrep.2017.04.037.
[51] J.K. Hobbs, E.J. Prentice, M. Groussin, V.L. Arcus, Reconstructed ancestral enzymes impose a fitness cost upon modern bacteria despite exhibiting favourable biochemical properties, J. Mol. Evol. 81 (2015) 110–120, https://doi.org/10.1007/s00239-015-9697-5.
[52] I. Ahmad, N. Nawaz, N.M. Darwesh, S. Ur Rahman, M.Z. Mustafa, S.B. Khan, et al., Overcoming challenges for amplified expression of recombinant proteins using *Escherichia coli*, Protein Expr. Purif. 144 (2018) 12–18, https://doi.org/10.1016/j.pep.2017.11.005.
[53] G.L. Rosano, E.A. Ceccarelli, Recombinant protein expression in *Escherichia coli*: advances and challenges, Front. Microbiol. 5 (2014) 172, https://doi.org/10.3389/fmicb.2014.00172.
[54] A.B. Stergachis, E. Haugen, A. Shafer, W. Fu, B. Vernot, A. Reynolds, et al., Exonic transcription factor binding directs codon choice and affects protein evolution, Science 342 (2013) 1367–1372, https://doi.org/10.1126/science.1243490.
[55] V. Presnyak, N. Alhusaini, Y.-H. Chen, S. Martin, N. Morris, N. Kline, et al., Codon optimality is a major determinant of mRNA stability, Cell 160 (2015) 1111–1124, https://doi.org/10.1016/j.cell.2015.02.029.
[56] S. Pechmann, J. Frydman, Evolutionary conservation of codon optimality reveals hidden signatures of cotranslational folding, Nat. Struct. Mol. Biol. 20 (2013) 237–243, https://doi.org/10.1038/nsmb.2466.
[57] O. Popa, T. Dagan, Trends and barriers to lateral gene transfer in prokaryotes, Curr. Opin. Microbiol. 14 (2011) 615–623, https://doi.org/10.1016/j.mib.2011.07.027.
[58] B. Kintses, O. Méhi, E. Ari, M. Számel, Á. Györkei, P.K. Jangir, et al., Phylogenetic barriers to horizontal transfer of antimicrobial peptide resistance genes in the human gut microbiota, Nat. Microbiol. 449 (2018) 811, https://doi.org/10.1038/s41564-018-0313-5.
[59] O. Cohen, U. Gophna, T. Pupko, The complexity hypothesis revisited: connectivity rather than function constitutes a barrier to horizontal gene transfer, Mol. Biol. Evol. 28 (2011) 1481–1489, https://doi.org/10.1093/molbev/msq333.
[60] W. Davids, Z. Zhang, The impact of horizontal gene transfer in shaping operons and protein interaction networks—direct evidence of preferential attachment, BMC Evol. Biol. 8 (2008) 23, https://doi.org/10.1186/1471-2148-8-23.
[61] L. Käll, A combined transmembrane topology and signal peptide prediction method, J. Mol. Biol. 338 (2004) 1027–1036, https://doi.org/10.1016/j.jmb.2004.03.016.
[62] T.N. Petersen, S. Brunak, SignalP 4.0: discriminating signal peptides from transmembrane regions, Nat. Methods 8 (2011) 785–786, https://doi.org/10.1038/nmeth.1701.
[63] J.A. Bilmes, Transmembrane topology and signal peptide prediction using dynamic bayesian networks, PLoS Comput. Biol. 4 (2008) e1000213, https://doi.org/10.1371/journal.pcbi.1000213.
[64] U. Brockmeier, M. Caspers, R. Freudl, A. Jockwer, T. Noll, T. Eggert, Systematic screening of all signal peptides from *Bacillus subtilis*: a powerful strategy in optimizing heterologous protein secretion in gram-positive bacteria, J. Mol. Biol. 362 (2006) 393–402, https://doi.org/10.1016/j.jmb.2006.07.034.
[65] R. Freudl, Signal peptides for recombinant protein secretion in bacterial expression systems, Microb. Cell Factories 17 (2018) 52, https://doi.org/10.1186/s12934-018-0901-3.
[66] B. Kacar, E. Garmendia, N. Tuncbag, D.I. Andersson, D. Hughes, Functional constraints on replacing an essential

gene with its ancient and modern homologs, mBio 8 (2017) e01276-17, https://doi.org/10.1128/mBio.01276-17.
[67] P.A. Lind, C. Tobin, O.G. Berg, C.G. Kurland, D.I. Andersson, Compensatory gene amplification restores fitness after interspecies gene replacements, Mol. Microbiol. 75 (2010) 1078–1089, https://doi.org/10.1111/j.1365-2958.2009.07030.x.
[68] L.J. González, R.A. Bonomo, Host-specific enzyme–substrate interactions in SPM-1 metallo-β-lactamase are modulated by second sphere residues, PLoS Pathog. 10 (2014) e1003817, https://doi.org/10.1371/journal.ppat.1003817.
[69] M. Berrazeg, S. Diene, L. Medjahed, P. Parola, M. Drissi, D. Raoult, et al., New Delhi metallo-beta-lactamase around the world: an eReview using Google maps, Euro Surveill. 19 (2014).
[70] X.-W. Jiang, H. Cheng, Y.-Y. Huo, L. Xu, Y.-H. Wu, W.-H. Liu, et al., Biochemical and genetic characterization of a novel metallo-β-lactamase from marine bacterium *Erythrobacter litoralis* HTCC 2594, Sci. Rep. 8 (2018) 803, https://doi.org/10.1038/s41598-018-19279-0.
[71] J. VanPelt, A. Bergstrom, Z. Cheng, R. Poth, M. Morris, O. Lahey, et al., Clinical variants of New Delhi metallo-β-lactamase are evolving to overcome zinc scarcity, ACS Infect. Dis. 3 (2017) 927–940, https://doi.org/10.1021/acsinfecdis.7b00128.
[72] M.-R. Meini, L.I. Llarrull, A.J. Vila, Evolution of metallo-β-lactamases: trends revealed by natural diversity and in vitro evolution, Antibiotics (Basel) 3 (2014) 285–316, https://doi.org/10.3390/antibiotics3030285.
[73] H.J. Atkinson, J.H. Morris, T.E. Ferrin, P.C. Babbitt, Using sequence similarity networks for visualization of relationships across diverse protein superfamilies, PLoS One 4 (2009) e4345, https://doi.org/10.1371/journal.pone.0004345.
[74] J.N. Copp, E. Akiva, P.C. Babbitt, N. Tokuriki, Revealing unexplored sequence-function space using sequence similarity networks, Biochemistry 57 (2018) 4651–4662, https://doi.org/10.1021/acs.biochem.8b00473.
[75] K.-H. Choi, A. Kumar, H.P. Schweizer, A 10-min method for preparation of highly electrocompetent *Pseudomonas aeruginosa* cells: application for DNA fragment transfer between chromosomes and plasmid transformation, J. Microbiol. Methods 64 (2006) 391–397, https://doi.org/10.1016/j.mimet.2005.06.001.
[76] S. Fournet-Fayard, B. Joly, C. Forestier, Transformation of wild type *Klebsiella pneumoniae* with plasmid DNA by electroporation, J. Microbiol. Methods 24 (1995) 49–54, https://doi.org/10.1016/0167-7012(95)00053-4.
[77] J.N. Zadeh, C.D. Steenberg, J.S. Bois, B.R. Wolfe, M.B. Pierce, A.R. Khan, et al., NUPACK: analysis and design of nucleic acid systems, J. Comput. Chem. 32 (2011) 170–173, https://doi.org/10.1002/jcc.21596.
[78] N.R. Markham, M. Zuker, DINAMelt web server for nucleic acid melting prediction, Nucleic Acids Res. 33 (2005) W577–W581, https://doi.org/10.1093/nar/gki591.
[79] R. Sabi, R. Volvovitch Daniel, T. Tuller, stAIcalc: tRNA adaptation index calculator based on species-specific weights, Bioinformatics 33 (2017) 589–591, https://doi.org/10.1093/bioinformatics/btw647.
[80] P.M. Sharp, W.H. Li, The codon adaptation index—a measure of directional synonymous codon usage bias, and its potential applications, Nucleic Acids Res. 15 (1987) 1281–1295.
[81] P.M. Sharp, W.-H. Li, Codon usage in regulatory genes in *Escherichia coli*does not reflect selection for "rare" codons, Nucleic Acids Res. 14 (1986) 7737–7749, https://doi.org/10.1093/nar/14.19.7737.
[82] S.P. Zhang, G. Zubay, E. Goldman, Low-usage codons in *Escherichia coli*, yeast, fruit fly and primates, Gene 105 (1991) 61–72.